Hydrogen-Bonded Multilayers of Thermoresponsive Polymers

Eugenia Kharlampieva, Veronika Kozlovskaya, Julia Tyutina, and Svetlana A. Sukhishvili*

Department of Chemistry and Chemical Biology, Stevens Institute of Technology, Hoboken, New Jersey 07030

Received July 29, 2005; Revised Manuscript Received October 8, 2005

ABSTRACT: Neutral temperature responsive polymers, such as poly(*N*-vinylcaprolactam) (PVCL) and poly(vinyl methyl ether) (PVME), were included in ultrathin films using layer-by-layer alternating adsorption of these polymers with poly(methacrylic acid) (PMAA) at low pH. The amounts of polymers adsorbed and ionization of carboxylic groups within a film were quantified using in situ FTIR-ATR (Fourier transform infrared spectroscopy by attenuated total reflection). The strength of interlayer adhesion provided through hydrogen-bonding interactions was inferred from the critical pH value (pH_{CR}) and critical ionization (α_{CR}) for multilayer decomposition which were pH_{CR} 6.2, α_{CR} 2% and pH_{CR} 6.95, α_{CR} 30% for PMAA/PVME and PMAA/PVCL films, respectively. When deposited onto porous support membranes, PMAA/PVME and PMAA/PVCL multilayers exhibited temperature-responsive changes in dye permeability. The transition occurred in a wide temperature range from 25 to 35 °C, reflecting lower cooperativity of the phase separation of PVME and PVCL chains included within the film. Finally, PMAA/PVME and PMAA/PVCL self-assembly was performed onto particulate substrates, producing capsules which hold promise as temperature-responsive containers for controlled delivery applications.

Introduction

Recent years have seen an increasing interest in endowing temperature-responsive properties to thin polymer films at solid surfaces when such films are exposed to aqueous environment. Temperature-responsive films afford control of adhesion, adsorption, and permeability by external stimuli and are, therefore, promising for separation and controlled delivery applications. Building blocks for such films include polymers that respond with large reversible change in hydrophilicity to small temperature changes, showing the phase transition of the polymer chains from solvated coiled to dehydrated globular states when temperature is increased above a lower critical solution temperature (LCST). Of specific interest for biomedical applications are water-soluble polymers with LCST close to physiological temperature. One of the most studied polymers of this type is poly(*N*-isopropylacrylamide) (PNIPAM) whose hydrogels have been explored for biomedical applications,[1,2] including controlled sorption and release of solutes,[3−5] control of enzyme activity,[6] or protein separation.[7,8] Copolymers of PNIPAM with alkyl methacrylate, acrylic acid, and other hydrophilic and hydrophobic monomers have also been explored as a means to control LCST[9,10] and, consequently, the temperature profile of drug permeation.[11−13] Networks of PNIPAM/polyacid have also been explored as pH-regulated drug delivery systems.[14]

Besides studies on bulk hydrogels, there is an increasing interest to use temperature-responsive polymers for surface modification. This strategy allows control of surface wetting and adhesion properties by changes in temperature and shows promise in applications for separation technologies. Both surface-attached monolytic PNIPAM or its copolymer hydrogels[15−18] and PNIPAM brushes[19−21] have shown promise for control of surface adhesion and separation applications as they endow a surface with the ability to alternate its hydrophilicity/hydrophobicity via temperature variations.[22]

Much less explored is the route of binding temperature-responsive polymers at surfaces by means of self-assembly. A powerful yet facile technique for surface modification is layer-by-layer (LbL) polymer deposition. Lyon and co-workers were the first who applied the LbL technique to self-assemble microgel particles at surfaces. The approach combines the advantages known for microgels such as high loading capacity and fast response with simplicity of procedure. Specifically, temperature-responsive poly(*N*-isopropylacrylamide)-*co*-acrylic acid microgels and polyallylamine were alternately deposited at a surface via electrostatic self-assembly[23] and produced films used to demonstrate pulsed, thermally triggered release of insulin[24] and doxorubicin.[25]

The LbL method has been applied by Akashi and coworkers for self-assembly of chemically activated sequential deposition of temperature responsive copolymers containing amino or carboxylic groups.[26,27] Such self-assembly produced chemical linkages between amino and carboxylic groups of a PNIPAM copolymer and poly(acrylic acid) or poly(vinylamine), respectively. Electrostatically self-assembled multilayers and capsules based on copolymers of PNIPAM with charged monomers, in which free PNIPAM segments provided the film's temperature responsiveness were described by Glinel et al.[28] Using PNIPAM copolymers, Jaber and Schlenoff have recently demonstrated reversibility of thermal modulation of ion transport within electrostatically assembled multilayers.[29]

In the present study we explore self-assembly and temperature response of poly(*N*-vinylcaprolactam) (PVCL) and poly(vinyl methyl ether) (PVME) which were self-assembled with poly(methacrylic acid) (PMAA) through hydrogen bonding. The structures of the polymers are shown in Scheme 1. Both PVCL and PVME have LCST close to body temperature, 36[30] and 35 °C,[31]

* To whom correspondence should be addressed.

10.1021/ma0516891 CCC: $30.25
Published on Web 11/10/2005

Scheme 1. Chemical Structures of PVCL (a) and PVME (b)

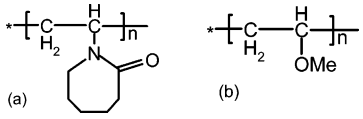

respectively, and are promising for biomedical applications.[32−34] In contrast to active research on PNIPAM, the number of studies carried out on PVCL and PVME is limited and largely focused on PVCL[35−39] and PVME[40−44] hydrogels and complexes in solutions. To our knowledge, LbL self-assembly of these polymers and temperature response of their films have not yet been reported, though dye-release properties of hydrogen-bonded self-assemblies of PNIPAM/PAA films at various temperatures has been explored earlier by Quinn and Caruso.[45,46] The main focus of this paper is to demonstrate, using a range of hydrogen-bonding polymer systems, the robustness of hydrogen-bonded self-assembly in binding temperature-responsive polymers at a surface and to explore the correlation between strength of intermolecular association, pH stability of multilayers, and their temperature response.

Experimental Section

Materials. Poly(methacrylic acid) (PMAA; M_w 150 000), poly(*N*-vinylpyrrolidone) (PVPON; M_w 55 000), poly(ethylene oxide) (PEO; M_w 200 000), poly(*N*-vinyl methyl ether) PVME (M_w 200 000) as 36.6% aqueous solution, poly(4-vinylpiridine) (PVP; M_w 200 000), 0.1 N hydrochloric acid, sodium hydroxide, dibasic and monobasic sodium phosphate, and ethyl bromide were purchased from Sigma-Aldrich. Poly(*N*-vinylcaprolactam) (PVCL; M_w 1800) was received from Polymer Source. All chemicals were used without any further purification. PVP was quaternized with ethyl bromide using well-established methods.[47] The produced polymer, Q90, contained 90% of quaternized units and was used for deposition of the precursor layer.

The SiO_2 template particles with diameter of 4.0 ± 0.2 μm were purchased from Polysciences Inc. as 10% aqueous dispersion. For in situ infrared experiments, we have used D_2O with 99.9% isotope content which was purchased from Cambridge Isotope Laboratories and used as received. For permeation experiments, a side-by-side horizontal diffusion glass cell from PermeGear with inner diameter of 9 mm and Anodisc 25 membranes from Whatman International with pore size of 0.02 μm and diameter of 25 mm were used. Thymol Blue (TB) supplied by Fisher Scientific was used as a permeant molecule. The H_2O used in all experiments was deionized and further purified by passage through a Milli-Q System (Millipore). Unless otherwise noted, 0.01 M phosphate buffer solutions were used to control pH. To create acidic media, 0.1 N hydrochloric acid was used to lower the pH of the buffer solution from 4.6 to 3.5. To create pH 2 media, 0.01 M aqueous solutions of hydrochloric acid were used.

Deposition of the Multilayers onto Si Substrates. For in situ FTIR-ATR studies, multilayers were prepared on the surface of an oxidized ATR silicon crystal using a procedure similar to that described in our earlier papers.[47] The silicon crystal was installed within a flow-through stainless steel cell. In a typical experiment, a Q90 layer, used as a precursor layer, was allowed to adsorb from a 0.1 mg/mL solution in 10^{-2} M phosphate buffer at pH 8.9, yielding an adsorbed amount of ~1.5 mg/m^2. After rinsing with the phosphate buffer at pH 8.9, a PMAA layer was deposited at the same high pH value of 8.9. This was followed by sequentially replacing the cell content with a 10^{-2} M phosphate buffer solution at pH 8.9 and pH 2. Subsequent multilayer deposition was done from 0.1 mg/mL polymer solutions at a constant pH of 2.

Deposition of Hydrogen-Bonded Multilayers for Permeability Measurements. Hydrogen-bonded multilayers were deposited on Anodisc 25 membranes using Robot Arm Catalyst 3 (CRS Robotics Corp.) and homemade software. The conditions for the multilayer deposition were chosen because of the pK_b value of aluminum oxide Anodisc membrane of 7.8.[48] Specifically, first PMAA layer was deposited from solution at pH 6.5 (instead of pH 8.9 used for deposition of multilayers on FTIR-ATR crystal) to provide electrostatic attraction between PMAA and the substrate. Subsequent deposition of PMAA/PVME, PMAA/PEO, PMAA/PVCL, or PMAA/PVPON films was performed at a constant pH 3.5. This pH was chosen since the aluminum oxide membrane surface did not provide sufficient adhesion to the film at lower pH values due to weakening of electrostatic binding between protonated PMAA and positive charges of the aluminum oxide surface at acidic pH values. The deposition was performed using 0.2 mg/mL aqueous polymer solutions and a deposition time of 20 min, with two rinsing steps in 10^{-2} M phosphate buffer solution at pH 3.5 applied between the polymer deposition steps. In all experiments, the LbL procedure was terminated after neutral polymer was self-assembled as an outermost layer.

Capsule Preparation. For all deposition steps, unless otherwise noted, 0.2 mg/mL polymer solutions and a typical deposition time of 15 min were used. During that time, adsorption at each deposition cycle reached saturation. Multilayers of PMAA/PVCL were deposited on silica particles at pH 2 starting from PVCL polymer layers. Silica particle surfaces have an abundant amount of silanol groups under those conditions. Each deposition cycle was followed by centrifugation of suspensions at 1200 rpm for 1 min, removal of supernatant, and redispersing particles in solution at pH 2. The procedure was repeated three times to ensure complete removal of excess polymer. In the case of PMAA/PVME, the above procedure resulted in severe coagulation of silica particles, which could be avoided by using different deposition conditions. First, self-assembly was performed at pH 4.0 (starting from the deposition of PVME) to provide slight ionization to PMAA chains. Second, PVME was allowed to adsorb from a more dilute 0.08 mg/mL polymer solution for a shorter time of 5 min. Finally, all polymer and buffer solutions used in deposition were precooled to 10 °C, and the temperature during all steps of polymer deposition steps was also kept at 10 °C.

In all cases, after a desired number of layers were deposited, silica cores were dissolved using 8% hydrofluoric acid (HF), yielding hollow polymeric capsules. Capsules of (PVCL/PMAA) were then repeatedly washed with 0.1 M HCl aqueous solution using centrifugation as a means to separate capsules from the washing solution. Capsules of (PVME/PMAA) were washed several times with a buffer solution at pH 4.

Permeability Measurements. Permeation studies were performed using a PermeGear horizontal side-by-side diffusion cell which was equipped with a magnetic stirrer (PermeGear Inc.). The diffusion cell was thermostated by pumping water at a constant temperature through the outer half-cells. Anodisc 25 support membranes with deposited multilayer films were inserted between the two half-cells. Donor and receptor half-cells were filled with 0.1 mg/mL (2.1×10^{-4} M) TB solution and with buffer solution at pH 3.5, respectively. The contents of both compartments were agitated at 60 rpm. After a certain time interval, dependent on the permeability rate of a solute through the polyelectrolyte membrane, the contents of the donor and the receptor cells were removed and replaced with 0.1 mg/mL TB solution and with a buffer solution, respectively. At each temperature, the procedure was repeated three times at three different time intervals. In all cases, the time required for reaching a constant solution temperature was at least 30 times shorter than that allowed for solute permeation. The data were used to determine the initial increase of solute concentration in the receiving cell $\Delta C_{r,t}$ per unit time, $\Delta C_{r,t}/\Delta t$. Since the decrease in the solute concentration in the donor cell was less than 1% in all experiments, the assumption of the constant $\Delta C_{r,t}/\Delta t$ was valid. The concentration of TB in the receptor cell was determined using UV−vis spectrophotometry using the extinction coefficient for TB of 15 270 abs units cm^{-1} M^{-1} as determined at λ_{max} = 437 nm for TB solutions in 10^{-2} M phosphate buffer at pH 3.5. The perme-

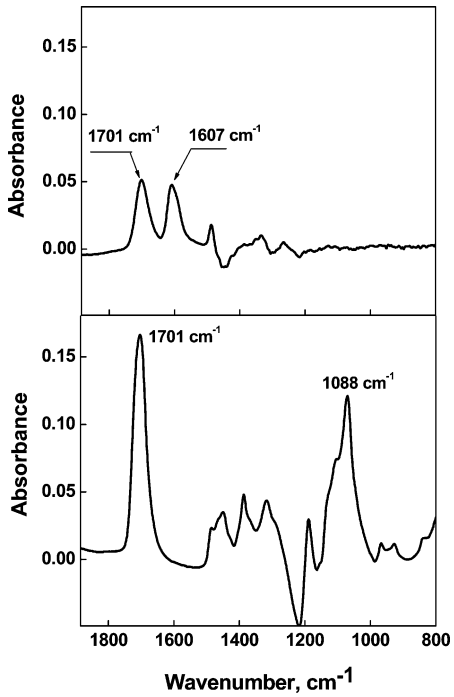

Figure 1. Representative FTIR-ATR spectra of the 8-layer PMAA/PVCL (top panel) and 8-layer PMAA/PVME with PMAA included into the top layers. Absorbance is plotted against wavenumber. Multilayer deposition and measurements were performed in D_2O solution whose pH was adjusted to pH 2. The spectra were obtained using a background spectrum collected using Si or Ge crystals coated with a precursor Q90 layer (for PMAA/PVCL and PMAA/PVME films, respectively), which were in contact with D_2O solution at pH 2.

ability coefficient, P, was calculated by using the following equation:

$$P = (\Delta C_{r,t}/\Delta t)V/(C_d A)$$

where C_d is the concentration of the solute in the donor cell (2.1×10^{-4} M), V is the volume of each half cell (3.4 mL), and A is the effective permeation area of the membrane (0.636 cm^2).

UV−vis Spectroscopy. Absorbance measurements were performed using an UV−vis spectrophotometer U-300 Hitachi (Hitachi International Inc.). Absorbance of all TB solutions was measured at the wavelength of 437 nm.

FTIR-ATR Measurements. The amounts of polymers adsorbed and the degree of ionization of the carboxylic groups were quantified by in situ FTIR-ATR using experimental protocols and calibration methods described earlier.[49] PMAA amounts adsorbed were quantified from the calibrated intensities of the vibrational bands of $-COO^-$ and $-COOH$ as described earlier.[50] Figure 2 shows representative FTIR-ATR spectra of 8-layer PMAA/PVCL (top panel) and 8-layer PMAA/PVME (bottom panel) films which were deposited in situ on the surface of Q90-pretreated Si and Ge ATR crystals, respectively. The spectrum of a PMAA/PVCL multilayer (top panel) shows two major peaks: an absorption band at 1701 cm^{-1} associated with stretch vibrations (C=O) of uncharged carboxylic groups of PMAA and a band centered at 1607 cm^{-1} from carbonyl stretch vibrations (CON) of the caprolactam ring. In the spectrum of PMAA/PVME multilayer (bottom panel), besides the peak of protonated PMAA at 1701 cm^{-1}, one sees a broad band centered at 1088 cm^{-1} associated with the presence of PVME within the film. A similar peak in the same region was observed for poly(ethylene oxide) (PEO) and was assigned to COC stretch vibrations.[54] The intensities of the peaks shown in Figure 1 were integrated by Galactic Grams/32 software. Note that for the same number of layers within the films the intensity of the PMAA vibrational band

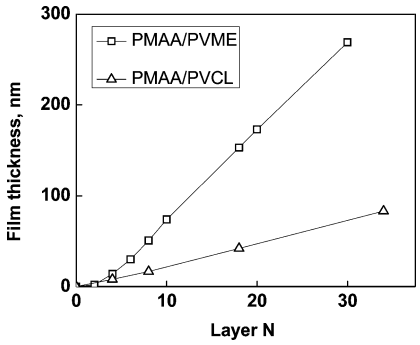

Figure 2. Layer-by-layer deposition of PMAA/PVCL (triangles) and PMAA/PVME (squares). The experiments were done at pH 2 and monitored via ellipsometry using a refractive index of 1.5.

(1701 cm^{-1}) is much higher when the poly(carboxylic acid) is included within the PMAA/PVME film (bottom panel) than those within the PMAA/PVCL (top panel), suggesting a much higher amount adsorbed for the PMAA/PVME film than for the PMAA/PVCL film.

Confocal Laser Scanning Microscopy. Confocal images of capsules were obtained with an LSM 5 PASCAL laser scanning microscope (Zeiss, Germany) equipped with C-Apochromat 63x/1.2 water immersion objective. Capsules were visualized through deposition of the FITC-labeled PMAA in the last two bilayers of capsules. The excitation wavelength was 488 nm.

Fluorescent Labeling of Poly(methacrylic acid). To visualize capsules for CLSM, labeling of PMAA was peformed as described elsewhere.[51] Specifically, PMAA (M_w = 150 000) was dissolved in 0.1 M phosphate buffer solution, and the solution pH was adjusted to 5.0 with 0.1 M sodium hydroxide solution. The polymer solution was mixed with of 1-ethyl-3-(3-(dimethylamino)propyl)carbodiimide hydrochloride and *N*-hydroxysulfosuccinimide sodium salt, 5 mg/mL each, and stirred for 30 min. The activation step was followed by addition of fluoresceinyl−ethylenediamine solution at pH = 6 with constant stirring for 10 h in darkness. Fluoresceinyl−ethylenediamine was synthesized as described earlier.[52] The labeled PMAA was dialyzed against phosphate buffer (pH 7, 0.1 M) for at least 7 days and then pure deionized water for 12 h. The molecular weight cutoff of dialysis tubing was 25 000. The dialysis was interrupted after no traces of fluorescence could be determined in the dialysis water. The dialyzed polymer solution was lyophilized, and 0.2 mg/mL solutions of labeled PMAA at pH = 2 were prepared and used for capsule preparation.

Scanning Electron Microscopy (SEM). SEM analysis was performed using a LEO 982 DSM instrument with a field emission gun at an operation voltage of 1 or 5 kV. Measurements were conducted after a drop of a particle suspension was applied to a precleaned silicon wafer and dried for 2 h.

Electron Energy-Loss Spectrometry (EELS). EELS thickness measurements were carried out using a 200 keV Philips CM20 field emission scanning transmission electron microscope with a Gatan 776 Enfina PEELS spectrometer. Hollow capsules were deposited from solution at pH = 1.0 onto a lacy-carbon gold TEM grid, dried, and cooled to −165 °C. The capsule wall thickness was derived at each point in a line scan across using the relation $I_0 = I_{total} \exp(-t/\lambda)$, where t is thickness, λ is the mean free path (MFP) for total inelastic electron scattering of the polymer, I_{total} is total and I_0 the zero-loss electron intensity,[53] and λ = 260 nm was based on independent measurements of polymers.

Preparation of Hydrogen-Bonded Multilayers on Silica Wafers. Hydrogen-bonded multilayers were deposited onto flat silica wafers. A precursor layer of Q-90 was deposited first onto silica wafers at pH 8.9 followed by two washings with buffers at pH = 8.9 and adsorption of the PMAA from solution at pH = 6.5 followed by washing with buffers at pH = 6.5 and 3.5. Then PVME/PMAA layers were self-assembled at pH = 3.5.

Table 1. Average Bilayer Thicknesses for Different Hydrogen-Bonded Multilayers Ellipsometrically Determined with Five-Bilayer Films

	ellipsometric bilayer thickness, nm	
polymer system	pH 2, no precursor layer	pH 3.5, with Q90 precursor layer
PMAA/PVME	15.6	15.1
PMAA/PVCL	4.8	5.4
PMAA/PVPON	4	3.8
PMAA/PEO	20	20.6

The washing cycles were performed at pH 2.0. The thickness measurements followed by drying of wafers with self-assembled polymers. To check whether the thickness of the layers changes with temperature increase, the wafers were immersed into the phosphate buffer solution at pH 3.5, heated to 35, 52, and 74 °C, and the thicknesses of layers were measured again.

Ellipsometry. Thickness measurements of self-assembled films were done using a custom-made phase-modulated ellipsometer. Before film deposition, silicon wafers were irradiated with UV light for 30 min, washed with distilled water, and treated with concentrated sulfuric acid for 15 min, followed by washing with distilled water and drying under a stream of compressed air.

Results and Discussion

PMAA/PVCL and PMAA/PVME Films on a Flat Substrate. The layer-by-layer deposition of PMAA/PVCL and PMAA/PVME was monitored by ellipsometry and in situ FTIR-ATR experiments. The deposition procedures are described in the Experimental Section. As seen in Figure 1, the FTIR-ATR spectra of the multilayers do not contain the 1552 cm^{-1} $-COO^-$ vibrational band, suggesting that PMAA is completely protonated under these conditions. Note that a priming polycation layer was used for depositing hydrogen-bonded films in FTIR-ATR experiments. However, we have also deposited multilayers at the surface of the oxidized silicon crystal without the precursor layer, relying on hydrogen bonding of protonated silanol groups and hydrogen-bonded polymer. In addition, to model multilayer growth onto Anodisk membrane, multilayers were also assembled onto a polycation-precoated silicon wafer surfaces at a higher pH of 3.5 using a polycation precursor layer. The deposition procedures are described in detail in the Experimental Section. Table 1 compares bilayer film thicknesses measured for the three cases described above. In addition to PMAA/PVCL and PMAA/PVME systems, poly(*N*-vinylpyrrolidone) (PMAA/PVPON) and poly(ethylene oxide) (PMAA/PEO) multilayer growth is also shown for comparison. For different deposition pH and regardless of the presence of a precursor layer, the amounts adsorbed determined by FTIR or ellipsometry for a particular system were always consistent within 1−10%. In our recent paper, we have reported on the effect of ionization within a precursor layer on the growth of weakly associated PMAA/PEO system.[54] Specifically, PMAA/PEO growth on particulate substrates at pH 3.5 was inhibited when a poly(ethylenimine) precursor layer was deposited at the pH used for film deposition. However, PMAA/PEO films could be grown on those substrates when the PEI precursor was allowed to adsorb at a pH value higher than that used for hydrogen-bonding deposition. Inhomogeneous structure and different charge of precursor-treated surface layers formed through the latter deposition route promoted further PMAA/PEO growth. In this work we deposited Q90 at pH 9 to prime the surface of silicon wafers with subsequent hydrogen-bonded multilayer growing performed at pH 3.5. Figure 2 also illustrates deposition of PMAA/PVCL and PMAA/PVME multilayers as a function of layer number at the surface of silicon wafers at pH 2. One can see a linear increase in deposited mass for both PMAA/PVME and PMAA/PVCL films at layer numbers higher than four. For PVCL systems, the incremental bilayer thickness was 4.8 nm, with the same mass in mg/m^2 of PMAA and PVCL deposited within each bilayer. This corresponds to ~1.6 molar excess of PMAA units—a value that is in good agreement with those (2.1 times molar excess of PMAA over PVPON) reported in our earlier work for hydrogen-bonded PVPON/PMAA multilayers.[56] The amount of PMAA/PVME deposited within a bilayer was about 4 times larger than in PMAA/PVCL films. Similarly thick films, with sharp increase in thickness starting from the fourth layer, were shown before for PMAA/PEO systems and contrasted with the robust deposition of PMAA/PVPON films.[55] The difference was explained by weaker intermolecular hydrogen bonding between PMAA and PEO molecules compared to PMAA and PVPON binding. Since PVCL can be considered as a homologue of PVPON, and PVME is related to PEO as both polymers contain ether groups, a similar argument for the smaller number of intermolecular hydrogen bonds between PVME with the polyacid explains the larger thickness of PMAA/PVME bilayers. Control experiments with deposition of PVCL with a larger molecular weight of 70 000 showed that the PVCL/PMAA bilayer thickness was largely independent of PVCL molecular weights, suggesting that the molecular weight effects cannot explain the observed large difference in amounts of polymers deposited in PMAA/PVME and PMAA/PVCL films.

We have shown earlier that, for hydrogen-bonded self-assemblies that involve poly(carboxylic acid)s, an increase in pH to a certain value results in dissociation of the polymer chains and film destruction.[56] The pH of film disintegrations determined as critical pH was directly correlated with critical ionization of PMAA and controlled by the strength of the hydrogen bonding. Figure 3 (top panel) shows the evolution of mass adsorbed when PMAA/PVME or PMAA/PVCL multilayers prepared at pH 2 were sequentially exposed to buffer solutions with increasingly high pH. Changes in ionization of the self-assembled polyacids during pH increase are shown in the bottom panel in Figure 3. The critical pH values were 6.2 and 6.95 for PMAA/PVME to PMAA/PVCL films, respectively. Increased film stability from PMAA/PVME to PMAA/PVCL systems was directly correlated with an increase in the critical amounts of the ionized carboxylic groups. The weakly bound PMAA/PVME complex can tolerate only ~2% ionization of PMAA, but PMAA/PVCL films dissolved when PMAA ionization was as high as 30%. Similar differences in strength of intermolecular interactions within hydrogen-bonded systems were also observed for PMAA/PEO and PMAA/PVPON films which dissolved at 1% and 14% PMAA ionization, respectively.[56] PMAA/PVCL films studied in this paper showed the highest stability among all hydrogen-bonded systems in similar conditions. Enhanced pH stability of PMAA/PVCL multilayers as compared to PVPON/PMAA systems correlates with the presence of two extra methyl groups in the caprolactam ring and points to significant contribu-

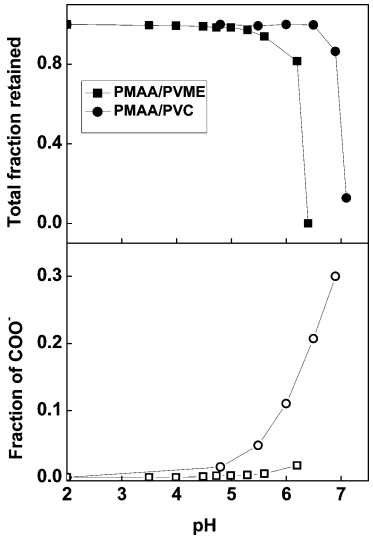

Figure 3. pH-triggered disintegration (top panel) and average ionization of PMAA (bottom panel) within 8-layer PMAA/PVME (squares) and PMAA/PVCL (circles) films monitored by in situ FTIR-ATR. The multilayers were deposited from D_2O solutions of 0.01 M phosphate buffer whose pH was adjusted to pH 2.

tion of hydrophobic interactions to film stabilization. Additional hydrophobic contribution to stabilization of hydrogen-bonded self-assembly is even more evident from comparison of the pH stability of PMAA/PVME films with earlier studies on PMAA/PEO systems. Specifically, more hydrocarbon moieties in PVME chains resulted in the shift of critical pH by about 1.6 units compared to PMAA/PEO whose dissociation occurred at pH 4.6. For complexation of hydrogen-bonding polymers with poly(carboxylic acid)s in aqueous solutions, additional contribution of hydrophobicity to macromolecular association has been much discussed in the literature. Specifically, using potentiometry and viscometry, Staikos et al. reported an increase in the complexation constant of PNIPAM with poly(acrylic acid) (PAA) at elevated temperatures.[56] Khutoryanskiy et al. also found temperature-enhanced aggregation of interpolymer complexes of several hydrogen-bonding polymers (including PAA/PVME)[43] that is consistent with the endothermic nature of interpolymer interactions in aqueous solutions. These data on complexation of polymer chains in solution are consistent with results on multilayer stability reported here and suggest that chain association is controlled to a large degree by the effects of water "caging" around interacting units and release of water molecules from hydrophobic hydration cages upon association, usually referred to as hydrophobic interactions. Specifically, this is relevant for complexation of temperature-responsive polymers which show significant hydrophobicity in aqueous solutions, especially at temperatures close to phase transition of the polymers in solution.

Permeability Studies. In this section, we present permeation studies of a small molecule through hydrogen-bonded films as a means to probe temperature responsiveness of self-assembled films. The central question to study was whether PVCL and PVME retain their temperature responsive properties after these polymers are included within self-assembled films. For these experiments, PMAA/PVCL or PMAA/PVME films as well as reference PEO/PMAA and PVPON/PMAA self-assembled films were deposited onto a supporting

Scheme 2. Chemical Structure of Thymol Blue

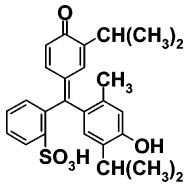

Anodisc 25 membrane with an average pore size of 0.02 μm, as described in the Experimental Section. The use of pH 3.5 for film deposition provided stability of a self-assembled film and its strong adhesion to the substrate. As inferred from in situ FTIR-ATR measurements, in all hydrogen-bonded systems (except for PMAA/PEO films) small ionization of PMAA in solution (~1−2%) at pH 3.5 was completely suppressed when PMAA was included within the film due to hydrogen bonding between carboxylic acid groups and proton-accepting moieties. In the PEO/PMAA system, the suppression of ionization was weak as a result of weak association between PEO and PMAA chains and the small fraction of carboxylic groups (~0.5 to 1%) ionized at this pH value. A permeant molecule, TB, whose structure is shown in Scheme 2 had pK_{a1} of 1.5 and did not interact with hydrogen-bonded films at pH 3.5 due to its negative charge at this pH value. The latter was demonstrated by in situ FTIR-ATR using PMAA/PVPON as an example. Another control experiment showed that permeability of the bare support membrane was not altered after having been coated with a single layer of PMAA (data not shown) in the wide temperature range from 15 to 50 °C.

When the number of layers deposited onto a PMAA-primed Anodisk membrane increased, the permeability of all films decreased at 25 °C, illustrating the bridging of membrane pores by adsorbed polymer chains and building a polymer film that retards TB diffusion (data not shown). Table 2 summarizes the permeability data for hydrogen-bonded multilayer films for several systems. The extent to which multilayers decreased diffusion of TB was dependent on the polymer system. For the same number of polymer layers deposited, systems in which hydrogen bonding occurred through ether group (PMAA/PEO and PMAA/PVME films) provided about 1 order of magnitude decrease in solute permeation rate, while deposition of PMAA/PVCL and PMAA/PVPON films resulted in about 2 or 3 orders of magnitude slower permeation of TB for a 10-layer films. Some authors reported much stronger decreases in diffusion of solute molecules of about 6 orders of magnitude for strongly bound PAH/PSS.[57,58] Qiu et al. have also shown that permeability of electrostatically bound multilayers can be further varied by a factor of several times by choosing different polymer pairs.[59] Because of multilayer deposition inside the cylindrical pores of the support membrane, the actual polymer layer thickness through which permeant molecules diffuse is usually poorly determined in such systems, and diffusion coefficients of permeant molecules using the relation $D \sim Pd$, where d is the membrane thickness, could not be calculated. However, data in Tables 1 and 2 allow us to make relative estimates of the TB diffusivity within multilayers. These values followed the ratio 1:5:40:380 for PMAA/PVCL, PMAA/PVPON, PMAA/PVME, and PMAA/PEO systems, respectively. One can see that PMAA/PEO multilayers demonstrated the highest intrinsic permeability to TB, indicating highly swollen and

Table 2. Permeability of 10-Layer Hydrogen-Bonded Multilayers Deposited at a Porous Anodisk 25 Support Membrane at pH 3.5 and 25 °C

polymer system	bare support membrane	PMAA/PVME 10L	PMAA/PEO 20L	PMAA/PVCL 10L	PMAA/PVPON 10L
TB permeability at 25 °C, cm/s	1.7×10^{-4}	1.2×10^{-5}	4.2×10^{-5}	8.0×10^{-7}	6.6×10^{-6}

easily permeable multilayer structure that results from weak association of PEO and PMAA chains. In contrast, PMAA/PVCL showed the smallest intrinsic permeability as a consequence of large number of intermolecular hydrogen bonds and additional hydrophobic interactions between them. Also note that the data on permeability are in good agreement with pH stability and critical ionization series for these hydrogen-bonded films discussed above.

Figure 4 contrasts the permeability of a supporting membrane coated with a 10-layer PMAA/PVME or PMAA/PVCL film. Apart from slower permeability of TB through the PMAA/PVCL film, one can see that in both cases a gradual increase in the multilayer permeability was observed in the temperature interval from 18 to 40 °C.

Temperature dependences of permeability for pairs of self-assembled polymers, PMAA/PVME vs PMAA/PEO and PMAA/PVCL vs PMAA/PVPON, are contrasted in Figure 5. One can see that while PMAA/PEO films showed moderate changes in permeability in the temperature interval 18−42 °C, PMAA/PVME films responded with a sharp increase in TB permeability in the temperature interval 25−35 °C, approaching permeability of the bare supporting membrane at temperatures higher than 35 °C. A similar trend is seen for different pairs of multilayers (PMAA/PVCL and PMAA/PVPON). This comparison shows that the observed increased permeation of TB through PMAA/PVME and PMAA/PVCL films is rooted in temperature-induced morphological changes of the films. Control experiments performed with PMAA/PVME and PMAA/PVCL films deposited onto silicon substrates at the same pH values showed that exposing hydrogen-bonded films to temperatures close to LCST (35 °C) in 10^{-2} M buffer solution at pH 3.5 for 6 h did not result in significant mass loss, which was always less than 7%. Thus, the small mass loss cannot explain the greatly increased permeability of PMAA/PVME and PMAA/PVCL films.

Evidently, an increase of permeation of TB through the films in the range of the LCST of PVCL or PVME reflected loosening of the film structure as a result of PVCL or PVME phase transitions. Note that both increased and decreased permeations were observed for films and surfaces modified with thermosensitive polymers. For example, Peng et al. reported that the direction of changes in the permeability of the PNIPAM-grafted porous membranes depended on the graft density of PNIPAM chains, with decreased permeability at high graft density of PNIPAM chains and vice versa. An increase in permeability in a membrane of cross-linked PNIPAM hydrogel above the LCST was reported by Liang et al.[18] However, hydrogels prepared by stepwise deposition and sequential reaction of PNIPAM-*co*-acrylic acid with poly(allylamine hydrochloride) showed suppression of ionic permeability above the LCST of PNIPAM because of shrinkage of polymer chains on the substrate.[27] We suggest that in our case when polymers were not covalently fixed within the film, deswelling of PVME or PVCL chains at temperatures near and above the LCST was accompanied by the appearance of voids in the multilayer film and an increase in dye permeability.

It is interesting to contrast the observed temperature-dependent behavior of PMAA/PVME and PMAA/PVCL films with the effect of intermolecular complexation of PVME and PVCL chains on their phase transition properties. Complexation of thermosensitive polymers with poly(carboxylic acid)s in solution was shown to significantly suppress thermoresponsive properties of these polymers.[60] Significant factors which have been shown to play an important role are the strength of intermolecular interactions and the composition of interpolymer complexes. Specifically, an increase in the polyacid content resulted in drastic suppression of cooperativity and the magnitude of the temperature response of PNIPAM chains in the polyacid/PNIPAM complexes.[61] For example, the temperature sensitivity of PVCL included in PMAA/PVCL complexes or PVCL-MAA copolymers was largely lost in systems with polyacid content r (calculated as molar ratio of polyacid units to those of a neutral polymer) as low as unity.[38]

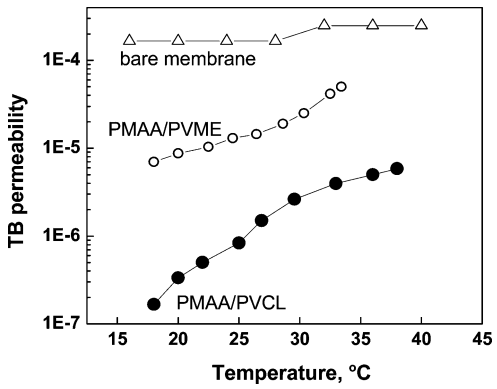

Figure 4. Permeability of TB molecules through 10-layer PMAA/PVME and PMAA/PVCL multilayers deposited on a porous Anodisk 25 support membrane at pH 3.5.

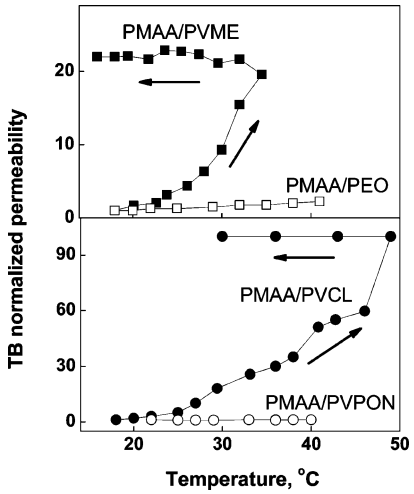

Figure 5. Temperature evolution of permeability of TB molecules, normalized to 18 °C, through 10-layer PMAA/PVME, PMAA/PEO, PMAA/PVCL, and PMAA/PVPON multilayers. Multilayers were deposited on a porous Anodisk 25 support membrane at pH 3.5 and exposed to increasing and then decreasing temperatures (see arrows).

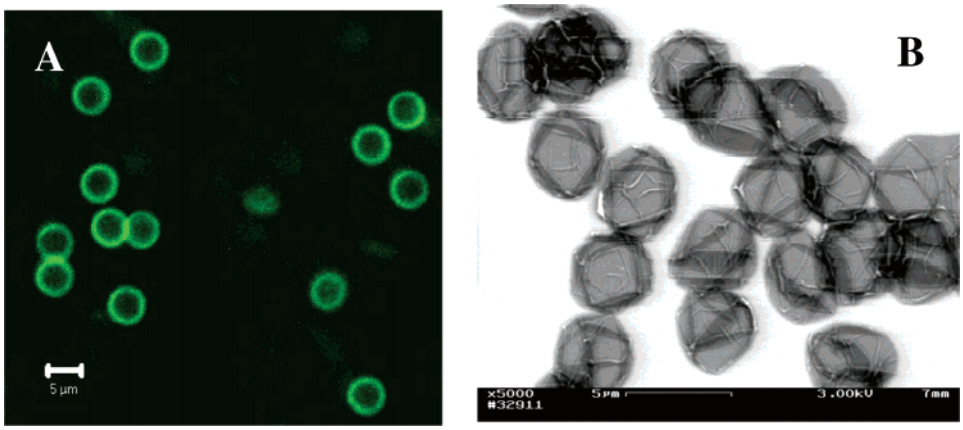

Figure 6. (A) CLSM image of $(PMAA/PVCL)_5$ capsule in solution at pH 2. (B) SEM image of the $(PMAA/PVCL)_5$ capsules after drying from water solution at pH 2. Capsules were produced using 4 μm silica particles.

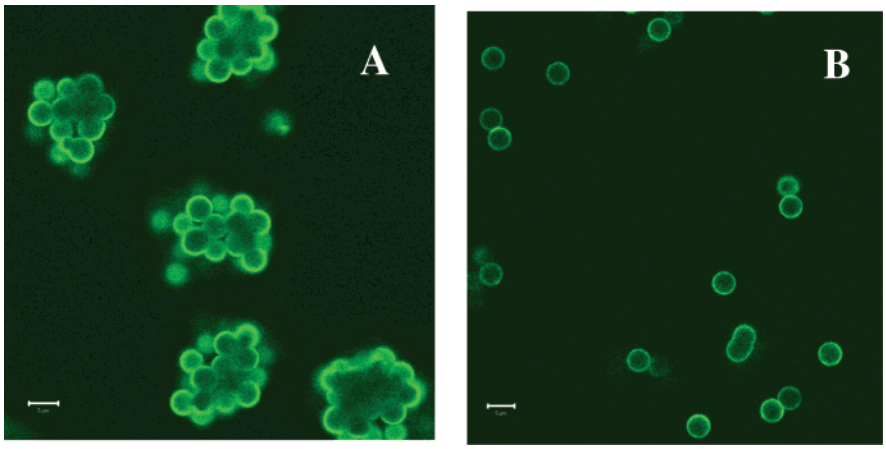

Figure 7. Comparison of the aggregation state of $(PMAA/PVME)_3$ capsules when they were prepared on silica cores using different deposition procedures. (A) CLSM image of $(PMAA/PVME)_3$ capsules produced on 4 μm silica core substrates from 0.2 mg/mL polymer solutions at pH 2 at room temperature with deposition time of 15 min. (B) CLSM of the $(PMAA/PVME)_3$ capsules solution produced on silica substrates at 10 °C using 0.08 mg/mL polymer solutions at pH 4 with 5 min deposition time. Scale bars are 5 μm for both images.

Similar effects were reported for PVME.[43] In our case, r was 0.45 for PMAA/PVME and 1.6 for PMAA/PVCL, and both systems showed temperature responsiveness. Small multilayer thickness and proximity of the solid substrate significantly contribute even when the film bridges the substrate's narrow pores, ~0.02 μm diameter, as free-standing film might account for the difference.

It is also evident from Figure 5 that the range in which the temperature response of PMAA/PVME and PMAA/PVCL multilayers occurs is wide, about 10−15 °C, while phase separation of PVME or PVCL in solution occurs in a narrow temperature region close to the LCST of the polymer solution. In polymer systems containing noninteracted groups of temperature-responsive polymers, such as in copolymers of vinylcaprolactam with a low content of acrylic acid in aqueous solutions at basic pH, temperature-induced phase separation occurs with high cooperativity in a narrow temperature interval. At the same time, a decrease of the phase transition temperature[61] and strong broadening of the transition[38,61] were observed when temperature-responsive moieties are hydrogen bonded with carboxylic groups in solutions at low pH values. These observations reflect hydrophobization of a polymer system caused by chain association. Broadening of the phase transition region reflected a decrease of the cooperativity of the phase transition and shortening of the average length of the temperature-responsive polymer sequences which are not bound to carboxylic groups and participate in the transition. Intermolecular binding within multilayer films also produces sequences of bound/unbound units which are intrinsically heterogeneous. Spatial constraints may account for broadening of the temperature transition region when temperature-responsive polymers are adsorbed[62] or grafted[20] onto solid surfaces, as well as for microgels containing cross-linked temperature-responsive polymers.[10] Within a multilayer of interacting chains of a temperature-sensitive polymer, a large density and broad distribution of these constraints (binding sites) are expected. Note that, for electrostatically assembled multilayers containing unbound PNIPAM sequences, a broad temperature range for changes in diameter of self-assembled hollow capsules[28] and for water uptake or loss by substrate-attached films[29] was reported.

Permeability of both PMAA/PVME and PMAA/PVCL films was not reversible (Figure 5). The data are consistent with irreversible morphological changes of PMAA/PVME and PMAA/PVCL due to the lack of permanent chemical cross-links within self-assembled films. In such films, initial mutual arrangements of polymer chains do not recover when temperature is lowered. Irreversibility of the film response does not diminish the potential interest of these films for controlled delivery applications, as in many cases a one-

Table 3. Comparison of Bilayer PMAA/PVME and PMAA/PVCL Thickness in Hollow Capsules As Determined by EELS and in the Flat Films As Measured with Ellipsometry[a]

polymer system	capsule wall thickness as determined by EELS, nm	ellipsometric thickness of films deposited at silicon wafer at pH 3.5, nm
PMAA/PVME	8 ± 2[b]	14 ± 2
PMAA/PVCL	5 ± 1	5 ± 1

[a] The data were averaged over at least 10 capsules for EELS measurements and over three samples with four measurements per sample for ellipsometric determination. [b] Capsules prepared at pH 4.0 with deposition time 5 min per layer using 0.08 mg/mL PVME concentration.

time controlled delivery is needed, such as in the case of delivery containers described below.

Toward Temperature-Responsive Capsules: PMAA/PVME and PMAA/PVCL Systems. While using silica particles as a core material, direct deposition of PMAA/PVCL or PMAA/PVME multilayers was possible without prior deposition of precursor layers. This occurred due to hydrogen-bonding interactions of silanol groups on silica surfaces with −C═O groups along PVCL chains or with ether group of PVME at low pH values. A typical confocal laser scanning microscopy image of hollow PMAA/PVCL capsules shown in Figure 6 (panel A) and a SEM image of dried capsules (panel B) show that nonaggregated capsules can be produced at ambient temperature and pH 2. However, the deposition of PVME layers induced strong coagulation of template particles when the self-assembly was done under these conditions. Comparison of the CLSM images of PMAA/PVCL (Figure 6, panel A) and PMAA/PVME capsules (Figure 7, panel A) shows that while PVCL-containing capsules can be easily produced on silica cores at pH 2 even at room temperature, PVME-containing capsules tend to coagulate and produce clusters which cannot be separated. We attributed this to high hydrophobicity of the PVME layers at temperature close to LCST of the polymer. Since PVME undergoes a phase transition at 35−36 °C, handling the test tubes during capsule preparation has probably resulted in an increase in suspension temperature and induced coagulation of the PVME-coated particles.

To minimize the coagulation of the PMAA/PVME-coated particles, we have introduced the following modifications into the multilayer deposition procedure: (1) multilayer deposition and subsequent washings were performed at +10 °C to keep PVME far below its LCST, (2) a deposition pH was increased to 4.0 to provide a slight negative charge to PMAA chains, and (3) the deposition time was reduced to 5 min to reduce the amount of the PVME adsorbed. Figure 7 (panel B) shows a CLSM image of $(PMAA/PVME)_3$ capsules in solution at pH 4 prepared at 10 °C. One can see that the capsules are mostly separated.

The differences in capsule preparation were directly reflected in capsule wall thicknesses as measured by electron energy-loss spectrometry. These data are summarized in Table 3. While bilayer thickness of PMAA/PVCL capsules whose preparation conditions were very close to those used for a flat substrate, PMAA/PVME capsule walls obtained with EELS were significantly thinner than films deposited on the flat substrate because of a higher pH value, lower PVME concentrations, and a shorter time allowed for PVME deposition used during PMAA/PVME capsule construction. Studies of temperature response of the produced capsules are underway.

In summary, we have demonstrated that layer-by-layer hydrogen-bonded films and capsules can be produced through self-assembly of a weak poly(carboxylic acid) and temperature responsive polymers such as PVME or PVCL. The permeability of such films to low molecular weight permeant molecules was observed but was significantly attenuated through interaction with the poly(carboxylic acid) chains, resulting in broadening of the temperature range of the phase transition. We demonstrate feasibility of preparation of hollow capsules based on PMAA/PVME and PMAA/PVCL which hold promise as temperature-responsive containers for controlled delivery applications. Work targeted to quantification of temperature response of such capsules is currently underway.

Acknowledgment. We thank Thomas Cattabiani (Stevens Institute of Technology) for many discussions.This work was supported by the National Science Foundation under Award DMR-0209439.

References and Notes

(1) Peppas, N.; Bures, P.; Leobandung, W.; Ichikawa, H. *Eur. J. Pharm. Biopharm.* **2000**, *50*, 27.
(2) Langer, R.; Peppas, N. *AIChE J.* **2003**, *49*, 2990.
(3) Hoffman, A.; Afrasiabi, A.; Dong, L. *J. Controlled Release* **1986**, *4*, 213.
(4) Bae, Y.; Okano, T.; Hsu, R.; Kim, S. *Macromol. Chem. Rapid Commun.* **1987**, *8*, 481.
(5) Hoffman, A. *Clin. Chem.* **2000**, *46*, 1478.
(6) Dong, L.; Hoffman, A. *J. Controlled Release* **1986**, *4*, 223.
(7) Hoffman, A.; Chen, G. *Bioconjugate Chem.* **1994**, *5*, 371.
(8) Takei, Y.; Aoki, T.; Sanui, K.; Ogata, N.; Okano, T.; Sakurai, Y. *Bioconjugate Chem.* **1993**, *4*, 42.
(9) Yin, S.; Stover, H. *Macromolecules* **2002**, *35*, 10178.
(10) Bradley, M.; Ramos, J.; Vincent, B. *Langmuir* **2005**, *21*, 1209.
(11) Okano, T.; Bae, Y.; Jacobs, J.; Kim, S. *J. Controlled Release* **1990**, *11*, 255.
(12) Yoshida, R.; Sakai, K.; Okano, T.; Sakurai, Y.; Bae, Y.; Kim, S. *J. Biomater. Sci., Polym. Ed.* **1991**, *3*, 155.
(13) Brazel, C.; Peppas, N. *J. Controlled Release* **1996**, *39*, 57.
(14) Zhang, J.; Peppas, N. *Macromolecules* **2000**, *33*, 102.
(15) Takei, Y. G.; Aoki, T.; Sanui, K.; Ogata, N.; Sakurai, Y.; Okano, T. *Macromolecules* **1994**, *27*, 6163.
(16) Kidoaki, S.; Ohya, S.; Nakayama, Y.; Matsuda, T. *Langmuir* **2001**, *17*, 2402.
(17) Harmon, M.; Kuckling, D.; Frank, C. *Macromolecules* **2003**, *36*, 162.
(18) Liang, L.; Feng, X.; Peurrung, L.; Viswanathan, V. *J. Membr. Sci.* **1999**, *162*, 235.
(19) Jones, D. M.; Smith, J. R.; Huck, W. T. S.; Alexander, C. *Adv. Mater.* **2002**, *14*, 1130.
(20) Zhang, G. *Macromolecules* **2004**, *37*, 6553.
(21) Okano, T.; Kikuchi, A.; Sakurai, Y.; Takei, Y.; Ogata, N. *J. Controlled Release* **1995**, *36*, 125.
(22) Yamada, N.; Okano, T.; Sakai, H.; Karikusa, Y.; Sawasaki, Y.; Sakurai, Y.; *Macromol. Chem. Rapid Commun.* **1990**, *11*, 571.
(23) Serpe, M.; Jones, C.; Lyon, L. *Langmuir* **2003**, *19*, 8759.
(24) Nolan, C.; Serpe, M.; Lyon, L. *Biomacromolecules* **2004**, *5*, 1940.
(25) Serpe, M.; Yarmey, K.; Nolan, C.; Lyon, L. *Biomacromolecules* **2005**, *6*, 408.
(26) Serizawa, T.; Nanameki, K.; Yamamoto, K.; Akashi, M. *Macromolecules* **2002**, *35*, 2189.
(27) Serizawa, T.; Matsukuma, D.; Nanameki, K.; Uemura, M.; Kurusu, F.; Akashi, M. *Macromolecules* **2004**, *37*, 6531.
(28) Glinel, K.; Sukhorukov, G.; Möhwald, H.; Khrenov, V.; Tauer, K. *Macromol. Chem. Phys.* **2003**, *204*, 1784.
(29) Jaber, J.; Schlenoff, J. *Macromolecules* **2005**, *38*, 1300.
(30) Yanul, N.; Kirsh, Y.; Anufrieva, E. *Therm. Anal. Calorim.* **2000**, *62*, 7.
(31) Maeda, Y. *Langmuir* **2001**, *17*, 1737.
(32) Galaev, I.; Mattiasson, B. *Trends Biotechnol.* **1999**, *17*, 335.

(33) Strukova, S.; Dugina, T.; Chistov, I.; Lange, M.; Markvicheva, E.; Kuptsova, S.; Zubov, V.; Glusa, E. *Clin. Appl. Thrombosis/Hemostasis* **2001**, *7*, 325.
(34) Vihola, H.; Laukkanen, A.; Hirvonen, J.; Tenhu, H. *Eur. J. Pharmacol. Sci.* **2002**, *16*, 69.
(35) Kuptsova, S.; Markvicheva, E.; Kochetkov, K.; Belokon, Y.; Rumsh, L.; Zubov, V. *Biocatal. Biotransform.* **2000**, *18*, 133.
(36) Meeussen, F.; Nies, E.; Berghmans, H.; Verbrugghe, S.; Goethals, E.; Prez, F. *Polymer* **2000**, *41*, 8597.
(37) Peng, S.; Wu, C. *Polymer* **2001**, *42*, 7343.
(38) Okhapkin, I.; Nasimova, I.; Makhaeva, E.; Khokhlov, A. *Macromolecules* **2003**, *36*, 8130.
(39) Yanul, N.; Kirsh, Y.; Verbrugghe, S.; Goethals, E.; Du Prez, F. *Macromol. Chem. Phys.* **2001**, *202*, 1700.
(40) Saito, S. *Colloids Surf.* **1986**, *19*, 351.
(41) Meeussen, F.; Bauwens, Y.; Moerkerke, E.; Niels, E.; Berghmans, H. *Polymer* **2000**, *41*, 3737.
(42) Maeda, Y.; Mochiduki, H.; Yamamoto, H.; Nishimura, Y.; Ikeda, I. *Langmuir* **2003**, *19*, 10357.
(43) Khutoryanskiy, V.; Nurkeeva, Z.; Mun, G.; Dubolazov, A. *J. Appl. Polym. Sci.* **2004**, *93*, 1946.
(44) Nies, E.; Ramzi, A.; Berghmans, H.; Li, T.; Heenan, R.; King, S. *Macromolecules* **2005**, *38*, 915.
(45) Quinn, J.; Caruso, F. *Langmuir* **2004**, *20*, 20.
(46) Quinn, J.; Caruso, F. *Macromolecules* **2005**, *38*, 3414.
(47) Kharlampieva, E.; Sukhishvili, S. *Langmuir* **2004**, *20*, 10712.
(48) Lyklema, J. *Fundamentals of Interface and Colloid Science*; Academic Press: San Diego, 1995; Vol. II, p 3.114.
(49) Kharlampieva, E.; Sukhishvili, S. A. *Langmuir* **2003**, *19*, 1235.
(50) Izumrudov, V.; Kharlampieva, E.; Sukhishvili, S. *Biomacromolecules* **2005**, *6*, 1782.
(51) Pristinski, D.; Kozlovskaya, V.; Sukhishvili, S. *J. Chem. Phys.* **2005**, *122*, 014907.
(52) Baynes, J.; Maxwell, J.; Rahman, K.; Thorpe, S. *Anal. Biochem.* **1988**, *170*, 382.
(53) Egerton, R. *Electron Energy-Loss Spectroscopy in the Electron Microscope*, 2nd ed.; Plenum Press: New York, 1996.
(54) Kozlovskaya, V.; Yakovlev, S.; Libera, M.; Sukhishvili, S. *Macromolecules* **2005**, *38*, 4828.
(55) Sukhishvili, S. A.; Granick, S. *Macromolecules* **2002**, *35*, 301.
(56) Staikos, G.; Karayanni, K.; Mylonas, Y. *Macromol. Chem. Phys.* **1997**, *198*, 2905.
(57) Antipov, A.; Sukhorukov, G.; Donath, E.; Möhwald, H. *J. Phys. Chem. B* **2001**, *105*, 2281.
(58) Ibarz, G.; Dahne, L.; Donath, E.; Möhwald, H. *Macromol. Rapid Commun.* **2002**, *23*, 474.
(59) Qiu, X.; Donath, E.; Möhwald, H. *Macromol. Mater. Eng.* **2001**, *286*, 591.
(60) Burova, T.; Grinberg, N.; Grinberg, V.; Kalinina, E.; Lozinsky, V.; Aseyev, V.; Holappa, S.; Tenhu, H.; Khokhlov, A. *Macromolecules* **2005**, *38*, 1292.
(61) Shtanko, N.; Lequieu, W.; Goethals, E.; Du Prez, F. *Polym. Int.* **2003**, *52*, 1605.
(62) Larsson, A.; Kuckling, D.; Schönhoff, M. *Colloids Surf. A: Physicochem. Eng. Aspects* **2001**, *190*, 185.

MA0516891